CHEMICAL & PHARMACEUTICAL BULLETIN

Vol. 31, No. 11 November 1983

Regular Articles

[Chem. Pharm. Bull. 31(11)3785—3795(1983)]

Oxidation of Glucose on Immobilized Glucose Oxidase: Trickle-Bed Reactor Performance[1)]

TOYOHISA TSUKAMOTO, SHUSHI MORITA, and JUTARO OKADA*

Faculty of Pharmaceutical Sciences, Kyoto University, Yoshida-Shimoadachi-cho, Sakyo-ku, Kyoto 606, Japan

(Received March 22, 1983)

The oxidation of D-glucose on immobilized enzyme catalyst was carried out in a trickle-bed reactor operated in a single-pass or batch-recycle manner. The catalyst, with β-D-glucose oxidase and catalase both immobilized on activated carbon, was prepared by the carbodiimide method. The experiments were performed at atmospheric pressure, 25 °C and pH = 5.5 (in 0.1 M acetate buffer).

The rate equation for this enzymatic reaction and the mass balance equations in the reactor are proposed. The experimental results were well explained by these equations. The important factors which influence the global rate of reaction are the liquid-solid contacting efficiency, the mass transfer of oxygen in the liquid (gas-liquid, liquid-solid and intraparticle) and the mutarotation of D-glucose. The batch-recycle trickle-bed reactor with low conversions per pass was found to be preferable.

Keywords——oxidation; glucose; mutarotation; glucose oxidase; immobilized enzyme catalyst; trickle-bed reactor; contacting efficiency; mass transfer

Increasing efforts have recently been made to develop immobilized enzyme reactors in which enzymes are fixed by a gel lattice matrix, by adsorption or by covalent linkage to supports, or are encapsulated.[2)] When three phases (gas, liquid and solid) are involved in an enzymatic reaction system, the use of a trickle-bed reactor, where gas and liquid streams flow concurrently downward over a fixed bed of the immobilized enzyme catalyst particles, is expected to be favorable.

In designing trickle-bed reactors, one should consider the effects of a number of factors which influence the global rate of reaction, such as the interaction between the intrinsic kinetics and the interphase and intraparticle mass transfer, the liquid-solid contacting efficiency, the hydrodynamic characteristics of the reactor, *etc.*[3)] In the case of fast reactions, the gas-phase reactant is generally the limiting substance because of its low solubility, so that its mass transfer is very important. At the surface which is not covered with liquid, the interphase mass transfer effects would be slight, so that this surface contributes dominantly to the global rate of reaction.[4)]

In our previous studies[5-7)] the oxidation of D-glucose to δ-D-gluconolactone on glucose oxidase bound to activated carbon was chosen as such a three-phase enzymatic reaction. The kinetics and the intraparticle mass transfer effects were investigated in a slurry reactor,[6)] and

the liquid-solid contacting efficiency was studied in a trickle-bed reactor operated in a differential manner.[7]

The objective of this work is to analyze the experimental data, for the same reaction system, obtained in a trickle-bed reactor operated in an integral manner. The mass balance equations for the reactants were integrated numerically by using the results obtained in our previous work and the available correlations, and the calculated results were compared with the data. The mutarotation of D-glucose was an additional factor, as well as the mass transfer of oxygen and the contacting efficiency, which influenced the global rate of reaction. Thus, a batch-recycle trickle-bed reactor system was devised for the more effective use of the catalyst; the conversion of D-glucose per pass was low and the recycled feed solution was almost re-saturated with oxygen in the reservoir.

Experimental

Preparation of Immobilized Enzyme Catalyst——The immobilized enzyme catalyst was prepared in the same manner as described in a previous paper.[5] The average particle size of activated carbon used for the support was 0.055 cm (28 to 32 mesh). For 100 g of activated carbon (dry weight basis), 7 g of β-D-glucose oxidase (EC 1.1.3.4, from *Aspergillus niger*, Sigma Chemical Company, 24300 units/g stated activity) and 2 g of catalase (EC 1.11.1.6, from bovine liver, Sigma Chemical Company, 2000 units/mg stated activity) were used. The physical properties of the immobilized enzyme catalyst and the reaction mixture are summarized in Table I.

Table I. Physical Properties of the Immobilized Enzyme Catalyst and Reaction Mixture

Catalyst	
Glucose oxidase content, wt%	7.0
Catalase content, wt%	2.0
Particle diameter, d_P, cm	0.055[a]
Pore volume, cm^3/g	0.991[b,c]
Solid phase density, ρ_S, g/cm^3	2.18[b,d]
Particle density, ρ_P, g/cm^3	0.69[b,c]
Bulk density, ρ_B, g/cm^3	0.382[b,c]
Porosity of particle, ε_P, −	0.684[b,d]
Void fraction of bed, ε_B, −	0.446[b,d]
Tortuosity factor, τ, −	2.5[e]
Reaction mixture[e,f]	
Density, ρ_L, g/cm^3	1.006
Viscosity, μ_L, g/(cm·s)	9.42×10^{-3}
Saturated concentration of oxygen, $C^*_{O_2}$, mol/cm^3	1.12×10^{-6}

a) 28 to 32 mesh. *b*) For activated carbon. *c*) Measured. *d*) Calculated.
e) Ref. 6). *f*) For 0.1 M D-glucose solution, at 25 °C and 1 atm.

Apparatus and Operating Procedure——(a) Slurry Reactor: The slurry reactor was used to determine the activity of the immobilized enzyme catalyst. The reactor dimensions and the operating procedure were the same as reported in a previous paper.[6]

(b) Trickle-Bed Reactor: Figure 1 represents a schematic diagram of the apparatus used for trickle-bed reactor operation. The glass reactor 1 was 2.1 cm i.d. and 60 cm long. In a constant temperature bath 4, 0.1 M D-glucose solution (in 0.1 M acetate buffer, pH = 5.5) contained in the reservoir 3 (20 l) was saturated with oxygen gas by continuous bubbling. The glucose solution and oxygen gas, which was circulating in the reactor system, were introduced into the top of the reactor, where the temperature was kept constant by circulating water from the constant temperature bath through the jacket. The glucose solution was introduced into the catalyst bed through a distributor consisting of three 0.1 cm i.d. and 1.0 cm long capillary tubes (stainless steel) placed across the reactor cross-section. The outlet of the tubes was located at 0.5 cm above the top of the prepacking. The immobilized enzyme catalyst bed was interposed between the pre- and after-packings of activated carbon particles of the same size as the catalyst. With this arrangement, the reaction mixture should be well distributed in the radial direction.[8] The lengths of the packing sections and the catalyst bed and other experimental conditions are listed in Table II.

After passing through the reactor, the effluent was separated into gas and liquid phases by means of the gas-liquid separator 7 located at the bottom of the reactor. In the separator, the liquid level was kept constant by the solenoid valve V, connected to a photo-electric switch. A part of the separated reaction mixture was fed into the top of a stripping column 5 for gas chromatographic analysis of oxygen dissolved in the liquid, and the rest was discharged through the solenoid valve. The stripping column and the analytical procedure were the same as those described in a previous paper.[5)]

The gas separated in the gas-liquid separator was circulated by the pump through a flask 8 immersed in the constant temperature bath. The volume of oxygen consumed in the reaction was measured by means of a gas burette 6. As shown in Fig. 1, the circulating gas was kept at atmospheric pressure by supplying oxygen gas from the burette.

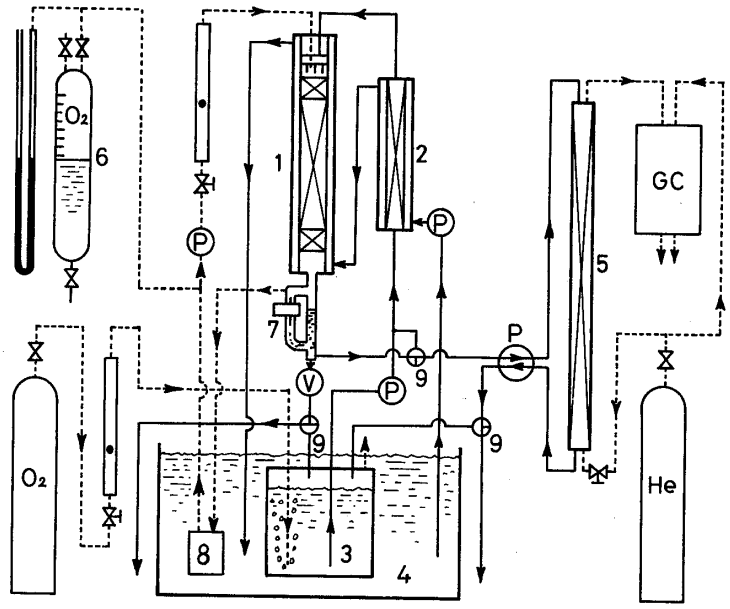

Fig. 1. Schematic Diagram of the Trickle-Bed Reactor Used

→, liquid flow line; --→--, gas flow line. 1, trickle-bed reactor; 2, heat exchanger; 3, reservoir; 4, constant temperature bath; 5, stripping column; 6, gas burette; 7, level controller; 8, flask; 9, three-way valve; P, pump; V, solenoid valve; GC, gas chromatograph.

TABLE II. The Experimental Conditions and Results

Operating mode	Single-pass			Batch-recycle
Run	SP-1	SP-2	SP-3	BR
Cross-sectional area of reactor, S, cm^2	3.46	3.46	3.46	3.40
Mass of catalyst in reactor, m, g	48.1	48.1	48.1	9.5
Length of catalyst section, z_t, cm	36.4	36.4	36.4	7.3
Length of pre- and after-packing section, cm	2.2	2.2	2.2	2.3
Superficial gas velocity, u_G, cm/s	3.6	3.6	3.6	3.7
Superficial liquid velocity, u_L, cm/s	0.039	0.127	0.333	0.123
Volume of liquid in the reservoir, V_R, cm^3	—	—	—	5000
Total liquid holdup,[a)] h_T, –	0.619	0.675	0.741	0.673
Liquid-solid contacting efficiency,[b)] f, –	0.701	0.737	0.821	0.734
Volumetric gas-liquid mass transfer coefficient,[c)] k_La_L, 1/s	0.0055	0.0141	0.0305	0.0140
Volumetric liquid-solid mass transfer coefficient,[d)] k_Sa_S, 1/s	0.309	0.559	0.906	0.550
Average rate of reaction, mol/(g·s), observed × 10^7	0.97	1.58	1.47	1.97[e)]
calculated × 10^7	0.92	1.55	1.72	2.11[e)]

a) Ref. 13). *b*) Ref. 7). *c*) Ref. 11). *d*) Ref. 12). *e*) At the beginning of the reaction ($t=0$).

The global rate of reaction, R [mol of oxygen/s], was calculated from the amount of oxygen consumed during a certain period, t_M [s];

$$R=\frac{M_{O_2}}{t_M}+\{(C_L)_{in}-(C_L)_{out}\}Q_L \quad (1)$$

where Q_L [cm^3/s] is the volumetric feed rate of reaction mixture, M_{O_2} [mol of oxygen] is the number of moles of oxygen gas supplied by the gas burette during t_M, C_L [mol/cm^3] is the concentration of oxygen in the bulk liquid and the subscripts "in" and "out" mean the inlet and outlet of the trickle-bed reactor, respectively. M_{O_2} was evaluated from the gas law.

(c) Batch-Recycle Trickle-Bed Reactor: The trickle-bed reactor (Fig. 1) was operated in a batch-recycle manner. In this case, an alternative trickle-bed reactor of shorter length (27 cm long and 2.1 cm i.d.) was used, and the effluents through the solenoid valve and stripping column were returned to the reservoir 3 (5 l). The operation was initiated by feeding fresh 0.1 M D-glucose solution (buffered) into the reactor. The global rate of reaction was measured at regular time intervals in the same manner as described in section (b). The conversion of δ-D-gluconolactone (product) could be evaluated from the measured R at any reaction time, since the reaction is completely selective. The operating conditions are given in Table II.

Results and Discussion

I. Activity of the Immobilized Enzyme Catalyst

When the external mass transfer resistances are negligible, the rate of reaction on the immobilized enzyme catalyst, R_P [mol of oxygen/(g·s)] can be expressed as[6]

$$R_P=\frac{\eta k_C C_L C_{\beta G}}{KC_L\left(1+\frac{C_P}{K_P}\right)+C_{\beta G}} \quad (2)$$

where η [−] is the catalyst effectiveness factor, $C_{\beta G}$ [mol/cm^3] and C_P [mol/cm^3] are the concentrations of β-D-glucose and δ-D-gluconolactone in the bulk liquid, respectively, k_C [cm^3/(g·s)] is the activity of catalyst, K [−] is the proportionality coefficient of the Michaelis constant for β-D-glucose, and K_P [mol/cm^3] is the product inhibition constant.

A large amount of the immobilized enzyme catalyst was prepared for this study, so it was necessary to check whether the new catalyst had the same activity as the previous one[6] or not. In the slurry reactor, the initial rate of reaction was measured at various concentrations of β-D-glucose and δ-D-gluconolactone. Since the Michaelis and product inhibition constants and the effective diffusivity of oxygen inside the catalyst pores were least affected by immobilization,[6] the reaction rate constant was estimated by least-squares analysis. The estimated value which gives the best fit (Fig. 2) was 3.1 [cm^3/(g·s)] and was considerably smaller than the value of 6.3 for the previous catalyst,[6] though the same procedure was employed for the catalyst preparation. The reason is not clear, but may be related to the difference in the scale

TABLE III. Kinetic Parameters[a]

Activity of the immobilized enzyme catalyst, k_C, cm^3/(g·s)	3.1
Proportionality coefficient of the Michaelis constant for β-D-glucose, K, −	46[b]
Product inhibition constant, K_P, mol/cm^3	6.2×10^{-5} [b]
Rate constant, k_α, l/s	1.48×10^{-4} [c]
Equilibrium constant, K_e, −	1.7[c]
Molecular diffusivity of oxygen in the liquid, D, cm^3/s	2.3×10^{-5} [d]
Effective diffusivity of oxygen in the liquid inside the pores, D_e, cm^2/s	6.3×10^{-6} [b]

a) At 25 °C and 0.1 M acetate buffer (pH=5.5). b) Ref. 6). c) Ref. 14).
d) Assumed to be identical with the molecular diffusivity of oxygen in water at 25 °C (ref. 15)).

of preparation (by a factor of about 100). In any event, this value of $k_C=3.1$ was used to analyze the present experimental results in the trickle-bed reactor. Other kinetic parameters are presented in Table III.

II. Trickle-Bed Reactor

(a) Mass Balance Equations——The fraction, f [−], of the particle surface covered with liquid is referred to as the contacting efficiency and is one of the most important factors which influence the global rate of reaction based on the mass of catalyst in a trickle-bed reactor, $(R_P)_{TB}$ [mol/(g·s)]. In the absence of the gas phase reaction, $(R_P)_{TB}$ is well expressed by[7,9]

$$(R_P)_{TB}=f(R_P)_{wet}+(1-f)(R_P)_{dry} \tag{3}$$

where $(R_P)_{wet}$ [mol/(g·s)] and $(R_P)_{dry}$ [mol/(g·s)] are the rates of reaction on the catalyst surfaces covered and not covered with the flowing liquid, respectively. Hereafter, the covered and not covered surfaces are referred to as the wet and dry surfaces, respectively.

The solubility of oxygen in the liquid is so low[5] that the limiting substance is considered to be oxygen, and the concentrations of β-D-glucose and δ-D-gluconolactone inside the pores can be regarded as identical with the respective concentrations in the flowing liquid. Considering the catalyst particles to be spherical, the mass balance equation in the steady state for oxygen inside the pores can be written as[6]

$$\frac{\partial^2 C_i}{\partial r^2}+\frac{2}{r}\frac{\partial C_i}{\partial r}-\frac{\rho_P}{D_e}\frac{k_C C_i C_{\beta G}}{KC_i\left(1+\frac{C_P}{K_P}\right)+C_{\beta G}}=0 \tag{4}$$

where C_i [mol/cm³] is the concentration of oxygen inside the pores, r [cm] is the radial distance in the particle, ρ_P [g/cm³] is the particle density, and D_e [cm²/s] is the effective diffusivity of oxygen in the liquid inside the pores.

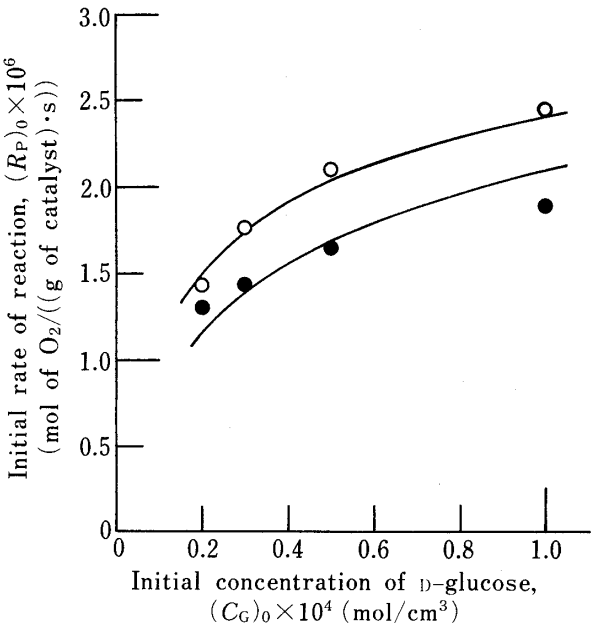

Fig. 2. Initial Rate of Reaction in the Slurry Reactor

Reaction temperature, 25 °C; pH, 5.5 (in 0.1 M acetate buffer); d_P [cm], 0.055; concentration of oxygen in the bulk liquid [mol/cm³], 1.12×10^{-6}; concentration of D-glucose [mol/cm³], 1.0×10^{-4}. Concentration of δ-D-gluconolactone [mol/cm³]: ○, 0; ●, 5.0×10^{-5}.

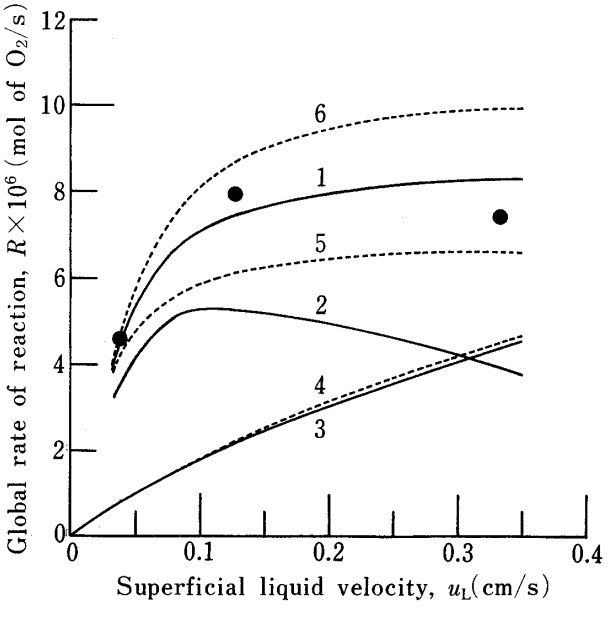

Fig. 3. Global Rate of Reaction in the Trickle-Bed Reactor *vs.* Superficial Liquid Velocity

Experimental conditions: see Table II. Observed global rate of reaction: ●. Calculated: 1, global rate of reaction; 2, rate of reaction on dry surface; 3, rate of reaction on wet surface; 4, global rate of reaction for complete wetting ($f=1$); 5, global rate of reaction for $1.1f$; 6, global rate of reaction for $0.9f$.

At the center of the particle, the gradient of oxygen concentration will be zero because of the symmetry, so that

$$\frac{\partial C_i}{\partial r}=0 \quad \text{at} \quad r=0 \tag{5}$$

Since the wet surface is covered with the liquid, the liquid-solid mass transfer resistance should be taken into account. On the other hand, in the case of dry surface there is no flowing liquid (there is considered to be no external mass transfer resistance), so that the liquid at the pore mouth is directly contacted with the flowing gas (pure oxygen) and can be considered to be in equilibrium with the gas. Then,

$$D_e\frac{\partial C_i}{\partial r}=k_S(C_L-C_S) \quad \text{at} \quad r=r_S \quad \text{for wet surface} \tag{6}$$

$$C_i=C^*_{O_2} \quad \text{at} \quad r=r_S \quad \text{for dry surface} \tag{7}$$

where r_S [cm] is the particle radius, C_S [mol/cm^3] is the concentration of oxygen at the wet surface of the catalyst particle, $C^*_{O_2}$ [mol/cm^3] is the saturated concentration of oxygen in the liquid, and k_S [cm/s] is the liquid-solid mass transfer coefficient.

When, in Eq. (3), the mass balances for oxygen in the pores under the wet and dry surfaces are assumed to be independent of each other, $(R_P)_{TB}$ can be written as

$$(R_P)_{TB}=f\frac{3D_e}{r_S\rho_P}\left(\frac{\partial C_i}{\partial r}\right)_{r=r_S,\,wet}+(1-f)\frac{3D_e}{r_S\rho_P}\left(\frac{\partial C_i}{\partial r}\right)_{r=r_S,\,dry} \tag{8}$$

The effect of axial dispersion on the concentration profile is assumed to be negligible.[10] Then, the mass balance for oxygen in the flowing liquid on the wet surface can be formulated by the following equation;

$$Q_L\frac{\partial C_L}{\partial z}=(k_La_L)S(C^*_{O_2}-C_L)-(k_Sa_S)S(C_L-C_S) \tag{9}$$

with

$$C_L=C^*_{O_2} \quad \text{at} \quad z=0 \tag{10}$$

where z [cm] is the axial distance from the top of the catalyst bed, S [cm^2] is the cross-sectional area of the reactor, and (k_La_L) [1/s] and (k_Sa_S) [1/s] are the gas-liquid and liquid-solid volumetric mass transfer coefficients, respectively.

In the D-glucose solution, α- and β-forms are in equilibrium;

$$\alpha\text{-D-glucose} \underset{k_\beta}{\overset{k_\alpha}{\rightleftarrows}} \beta\text{-D-glucose}$$

and

$$K_e=k_\alpha/k_\beta \tag{11}$$

where k_α [1/s] and k_β [1/s] are the first-order rate constants, and K_e [$-$] is the equilibrium constant. When the reaction is initiated with D-glucose (without product), the following mass balance holds in the reaction mixture;

$$(C_G)_0=C_{\alpha G}+C_{\beta G}+C_P \tag{12}$$

where $(C_G)_0$ [mol/cm^3] is the initial concentration of D-glucose (α- and β-forms; both are equilibrated at the beginning).

Since the concentrations of β-D-glucose or δ-D-gluconolactone in the flowing liquid and inside the pores can be regarded as the same at a fixed distance z, the mass balance equations

for these substances in the reactor can be expressed as

$$\frac{Q_L}{S}\frac{\partial C_{\beta G}}{\partial z}=-2(R_P)_{TB}\rho_B+h_T\{k_\alpha C_{\alpha G}-k_\beta C_{\beta G}\} \tag{13}$$

$$\frac{Q_L}{S}\frac{\partial C_P}{\partial z}=2(R_P)_{TB}\rho_B \tag{14}$$

with

$$(C_{\beta G})_{in}=\frac{K_e}{1+K_e}(C_G)_0 \quad \text{and} \quad (C_P)_{in}=0 \quad \text{at} \quad z=0 \tag{15}$$

where ρ_B [g/cm^3] is the bulk density of the bed, h_T [−] is the total liquid holdup in the trickle-bed reactor (the sum of the static holdup, h_S [−], and dynamic holdup, h_D[−]), and the subscript TB means the trickle-bed reactor. Putting k_m ($=k_\alpha+k_\beta$) [1/s] as the mutarotation constant, Eq. (13) can be converted into Eq. (13′).

$$\frac{Q_L}{S}\frac{\partial C_{\beta G}}{\partial z}=-2(R_P)_{TB}\rho_B+h_T[k_m\{(C_{\beta G})_{in}-C_{\beta G}\}+k_\alpha\{(C_P)_{in}-C_P\}] \tag{13′}$$

(b) Trickle-Bed Reactor Runs——The results are shown in Fig. 3. It is interesting to note that the global rate of reaction does not increase very much in the higher region of superficial liquid velocity, u_L [cm/s], though the mass transfer resistances decrease with u_L.

To analyze these results, the aforementioned mass transfer equations were used with the following correlations for (k_La_L)[11] and (k_Sa_S);[12]

$$k_La_L=0.0062\,{d_P}^{-0.5}\,{u_L}^{0.8}\,{u_G}^{0.8} \tag{16}$$

$$k_Sa_S=1.8{a_t}^2\left(\frac{u_L\rho_L}{\mu_La_t}\right)^{1/2}\left(\frac{\mu_L}{\rho_LD}\right)^{1/3} \tag{17}$$

where d_P [cm] is the particle diameter, u_G [cm/s] is the superficial gas velocity, D [cm^2/s] is the molecular diffusivity of oxygen in the liquid, ρ_L [g/cm^3] and μ_L [g/(cm·s)] are the density and viscosity of the liquid, respectively. a_t [1/cm] is the geometrical surface area of the particle per unit bed volume and can be written as

$$a_t=6(1-\varepsilon_B)/d_P \tag{18}$$

where ε_B [−] is the void fraction of the bed. The effective liquid-solid interfacial area per unit bed volume, a_S [1/cm], can be calculated as the product of f and a_t:

$$a_S=f\cdot a_t \tag{19}$$

Substituting Eq. (18) into Eq. (19), and dividing k_Sa_S by the resulting a_S gives k_S:

$$k_S=\frac{(k_Sa_S)}{6f(1-\varepsilon_B)} \tag{20}$$

The dynamic and static holdups (h_D and h_S) were estimated from the available correlations.[10b,13]

In our previous paper,[7] the value of f was presented as a function of d_P, u_L and u_G. Under fixed operating conditions, f is regarded as uniform throughout the catalyst bed.

The global rate of reaction in the reactor can be written as

$$R=\frac{m}{z_t}\int_0^{z_t}(R_P)_{TB}\partial z \tag{21}$$

where m [g] is the mass of catalyst in the bed and z_t [cm] is the length of the catalyst bed.

Equations (4), (8), (9), (13), (14) and (21) were integrated numerically with the initial and boundary conditions mentioned above. The physical properties, kinetic parameters, operating variables, *etc.*, all used for calculations, are summarized in Tables I to III.

The calculated curve for R (curve 1 in Fig. 3) agrees well with the experimental results. The rates on the dry and wet surfaces are also shown in the figure by curves 2 and 3, respectively. Though the fraction of dry surface is 20—30% under our experimental conditions, the rate on the dry surface is much larger than that on the wet surface, especially at low u_L. With increasing u_L, the contacting efficiency increases and the external mass transfer resistances decrease. Then, the rate on the wet surface increases monotonously, whereas the rate on the dry surface passes through a maximum value. When the catalyst surface is supposed to be completely covered with the flowing liquid ($f=1$), the calculated global rate of reaction (curve 4) is not very different from curve 3. This indicates that the dry surface contributes greatly to the global rate of reaction in the trickle-bed reactor even when no gas-phase reaction takes place. Calculations by changing only the value of f by $\pm 10\%$ give substantially higher and lower rates (curves 5 and 6). This may indicate that the values of f presented in the previous paper[7] are accurate and reliable.

(c) Concentration Profiles in the Trickle-Bed Reactor——It is worthwhile to know how the concentrations of both reactant and product vary with the bed length, because the reactor efficiency is highly dependent on the concentration profiles in the reactor. For the low and high liquid velocities employed in this study, the calculated results are shown in Fig. 4.

At low u_L (Fig. 4(a)), the oxygen concentration in the flowing liquid decreases rapidly near the entrance of the catalyst bed, because the enzymatic reaction is much faster than the mass transfer of oxygen. Near the exit of the bed, the β-D-glucose concentration approaches zero and the product concentration increases slightly, resulting in an increase of oxygen concentration. On the other hand, the α-D-glucose concentration decreases slightly (less than 10%) per pass through the reactor, due to the slower rate of mutarotation.

At high velocity (Fig. 4(b)), the oxygen concentration is rather high and becomes nearly constant after 10 cm. The α-D-glucose concentration can be seen to be unchanged (less than 0.3% conversion), whereas the β-D-glucose and product concentrations continue to change.

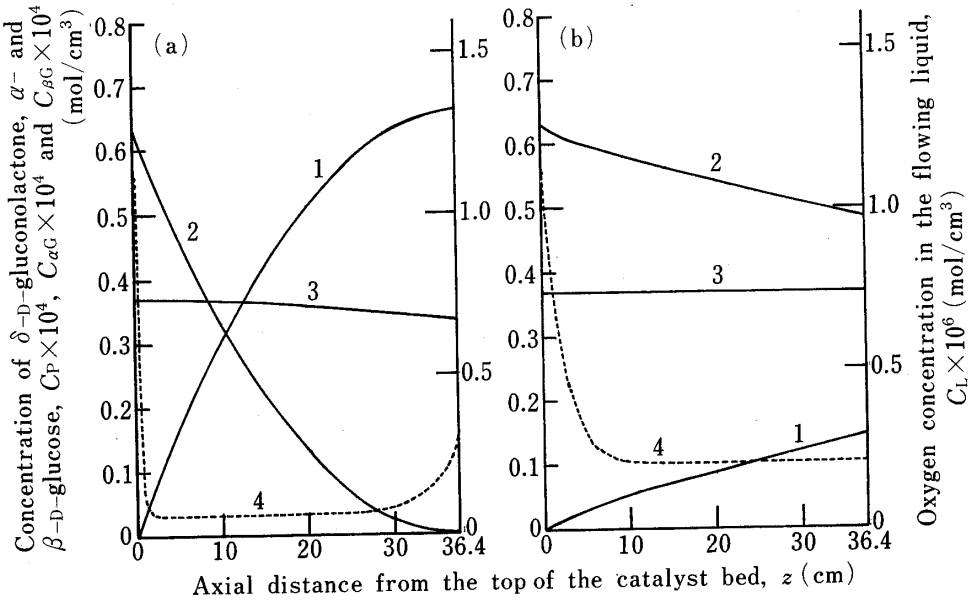

Fig. 4. The Calculated Concentration Profiles in the Trickle-Bed Reactor at $u_L=0.039$ cm/s (a) and $u_L=0.333$ cm/s (b)

1, δ-D-gluconolactone; 2, β-D-glucose; 3, α-D-glucose; 4, oxygen in the bulk liquid.

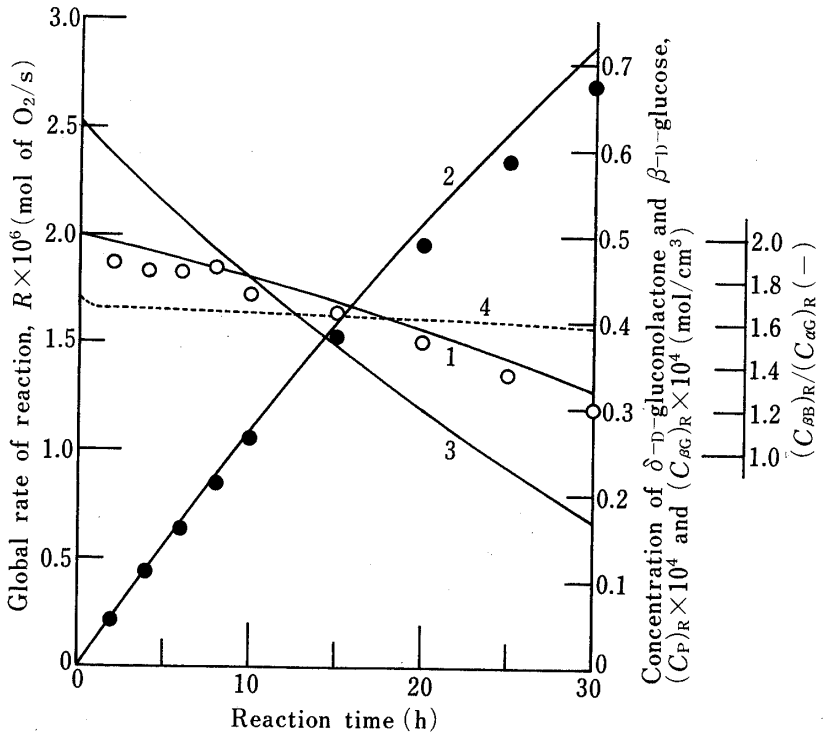

Fig. 5. The Global Rate of Reaction and the Concentrations of δ-D-Gluconolactone and β-D-Glucose in the Reservoir as a Function of Time in the Batch-Recycle Trickle-Bed Reactor System

Experimental conditions: see Table II. Observed: ○, global rate of reaction; ●, δ-D-gluconolactone. Calculated: 1, global rate of reaction; 2, δ-D-gluconolactone; 3, β-D-glucose; 4, $(C_{\beta G})_R/(C_{\alpha G})_R$.

This is due to the shorter residence time of the flowing liquid.

From these results and discussion, a batch-recycle trickle-bed reactor of shorter length, in which the liquid is flowing at medium velocity, is considered to be preferable. In this type of reactor, the effluent from the trickle-bed reactor would be re-saturated with oxygen and the equilibrium between α- and β-D-glucose would be almost reached in the reservoir.

III. Batch-Recycle Trickle-Bed Reactor Run

This run was carried out under the reaction conditions presented in Table II. The global rate of reaction in the trickle-bed reactor and the concentration of δ-D-gluconolactone in the reservoir are shown in Fig. 5 as a function of reaction time. The product concentration was evaluated numerically by summing the amount of oxygen consumed.

Because the volume of the liquid in the reservoir, V_R [cm^3], was much larger than the residual liquid volume (the sum of the liquid volumes in the flow line and in the trickle-bed reactor) and the liquid in the reservoir was considered to be perfectly mixed by introducing oxygen by continuous bubbling, the mass balance equations for β-D-glucose and δ-D-gluconolactone in the reservoir can be written as

$$\frac{\partial(C_{\beta G})_R}{\partial t}=-\frac{Q_L}{V_R}\{(C_{\beta G})_R-(C_{\beta G})_{out}\}+k_m\{(C_{\beta G})_0-(C_{\beta G})_R\}+k_\alpha\{(C_P)_0-(C_P)_R\} \quad (22)$$

$$\frac{\partial(C_P)_R}{\partial t}=-\frac{Q_L}{V_R}\{(C_P)_R-(C_P)_{out}\} \quad (23)$$

where the subscripts R and 0 mean the reservoir and the initial value, respectively, and t [s] is the reaction time. The initial conditions for Eqs. (22) and (23) are

$$(C_{\beta G})_R=(C_{\beta G})_{in}=(C_{\beta G})_{out}=\frac{K_e}{1+K_e}(C_G)_0 \quad \text{at} \quad t=0 \tag{24}$$

$$(C_P)_R=(C_P)_{in}=(C_P)_{out}=0 \quad \text{at} \quad t=0 \tag{25}$$

The liquid in the reservoir may be saturated with oxygen, so that

$$(C_L)_R=(C_L)_{in}=C^*_{O_2} \quad \text{at any} \quad t \tag{26}$$

Simultaneous integration of Eqs. (22) and (23) and all the mass balance equations described in the previous section II(a) and II(b) was performed numerically by converting only the initial conditions (15) into

$$(C_{\beta G})_{in}=(C_{\beta G})_R \quad \text{and} \quad (C_P)_{in}=(C_P)_R \quad \text{at} \quad z=0 \tag{27}$$

The calculated results shown in Fig. 5, are in good agreement with the experimental results. The calculated average rate of reaction, or the reactor efficiency, is shown in Table II. The reactor efficiency for the batch-recycle trickle-bed reactor is highest among them. As shown in Fig. 5, after 1 h the $C_{\beta G}/C_{\alpha G}$ ratio in the reservoir is nearly constant and about 1.6. Note that under our experimental conditions the ratio is 1.7 at equilibrium.[14] Since the retention time (V_R/Q_L) of the reaction mixture in the reservoir was about 3.3 h, the equilibration between α- and β-D-glucose and the re-saturation of oxygen were considered to be nearly completed. Also, the length of the trickle-bed reactor was so short that the oxygen conversion per pass was not very large and the $C_{\beta G}/C_{\alpha G}$ ratio did not appreciably decrease. These factors resulted in the higher average rate of reaction per unit mass of catalyst, *i.e.*, more effective use of the catalyst.

Conclusions

The oxidation of D-glucose was carried out in a trickle-bed reactor packed with immobilized glucose oxidase on activated carbon particles. The conclusions to be drawn from the experiments are as follows;

(1) The combined mass transfer and reaction for oxygen inside the catalyst pores may be expressed by Eq. (4), where the concentrations of β-D-glucose and δ-D-gluconolactone are regarded as equal to those in the bulk liquid.

(2) The global rate of reaction based on the mass of catalyst can be expressed as the sum of the rates on dry and wet surfaces (Eq. (8)).

(3) The axial and radial dispersion in the reactor could be neglected, and the mass balances for oxygen, β-D-glucose and δ-D-gluconolactone may be expressed by Eqs. (9), (13) and (14), respectively.

(4) The important factors which predominantly influence the reactor efficiency are the liquid-solid contacting efficiency, the mass transfer of oxygen (external and intraparticle) and the mutarotation of D-glucose.

(5) A trickle-bed reactor operated in a batch-recycle manner with low conversion per pass is considered to be preferable for this reaction.

References and Notes

1) A part of this work was presented at the 102nd Annual Meeting of the Pharmaceutical Society of Japan, Osaka, April 1982.
2) O. R. Zaborsky, "Immobilized Enzymes," CRC Press, Cleveland, Ohio, 1973; I. Chibata (ed.), "Koteika Koso," Kodansha Scientific, Tokyo, 1975; K. Mosbach (ed.), "Methods in Enzymology," Vol. 44, Academic Press, New York, 1976; I. Chibata, "Immobilized Enzymes," Kodansha Ltd., Tokyo, 1978; S. Fukui, I.

Chibata, and S. Suzuki (eds.), "Koso Kogaku," Tokyo Kagaku Dojin, Tokyo, 1981.
3) C. S. Tan and J. M. Smith, *AIChE J.*, **28**, 190 (1982); S. Goto, A Lakota, and J. Levec, *Chem. Eng. Sci.*, **36**, 157 (1981); P. L. Mills and M. P. Dudukovic, *ibid.*, **35**, 2267 (1980); O. M. Martinez, G. F. Barreto, and N. O. Lemocoff, *ibid.*, **36**, 901 (1981).
4) P. L. Mills and M. P. Dudukovic, *AIChE J.*, **27**, 893 (1981); H. H. Lee and J. M. Smith, *Chem. Eng. Sci.*, **37**, 223 (1982); M. Herskowitz, *ibid.*, **36**, 1665 (1981).
5) T. Tsukamoto, S. Morita, and J. Okada, *Chem. Pharm. Bull.*, **30**, 782 (1982).
6) T. Tsukamoto, H. Nomura, S. Morita, and J. Okada, *Chem. Pharm. Bull.*, **31**, 3377 (1983).
7) T. Tsukamoto, S. Morita, and J. Okada, *Chem. Pharm. Bull.*, **30**, 1539 (1982).
8) M. Herskowitz and J. M. Smith, *AIChE J.*, **24**, 439 (1978).
9) S. Morita and J. M. Smith, *Ind. Eng. Chem. Fundam.*, **17**, 113 (1978).
10) *a*) F. Turek and R. Lange, *Chem. Eng. Sci.*, **36**, 569 (1981); *b*) S. Goto and J. M. Smith, *AIChE J.*, **21**, 706 (1975).
11) Y. Sato, T. Hirose, F. Takahashi, and M. Toda, The 1st Pacific Chem. Eng. Congr., Paper 8-3, (1972).
12) D. W. Van Krevelen and J. T. C. Krekels, *Recl. Trav. Chim.*, **67**, 512 (1948).
13) C. N. Satterfield and P. F. Way, *AIChE J.*, **18**, 305 (1972).
14) F. Gram, J. A. Hveding, and A. Reine, *Acta Chem. Scand.*, **27**, 3616 (1973); Y. Inoue, "Toushitsu no Kagaku," Baifukan Publications Co., Tokyo, 1976, p. 97.
15) D. M. Himmelblau, *Chem. Rev.*, **64**, 527 (1964).